AMERICAN SOCIETY FOR MICROBIOLOGY | Infection and Immunity®

BACTERIAL INFECTIONS

The Enhancer-Binding Protein MifR, an Essential Regulator of α-Ketoglutarate Transport, Is Required for Full Virulence of *Pseudomonas aeruginosa* PAO1 in a Mouse Model of Pneumonia

Weichuan Xiong,[a,c] Alexander Perna,[a] Ikechukwu B. Jacob,[a,b] Benjamin R. Lundgren,[d] Guirong Wang[a,b]

[a]Department of Surgery, State University of New York (SUNY) Upstate Medical University, Syracuse, New York, USA
[b]Department of Microbiology and Immunology, State University of New York (SUNY) Upstate Medical University, Syracuse, New York, USA
[c]Department of Respiratory and Critical Care Medicine, The First Affiliated Hospital of Nanchang University, Nanchang, Jiangxi, People's Republic of China
[d]Department of Biology, The College of New Jersey, Ewing, New Jersey, USA

ABSTRACT The opportunistic human pathogen *Pseudomonas aeruginosa* PAO1 has an extensive metabolism, enabling it to utilize a wide range of structurally diverse compounds to meet its nutritional and energy needs. Interestingly, the utilization of some of the more unusual compounds often associated with a eukaryotic-host environment is regulated via enhancer-binding proteins (EBPs) in *P. aeruginosa*. Whether the utilization of such compounds and the EBPs involved contribute to the pathogenesis of *P. aeruginosa* remains to be fully understood. To narrow this gap, we investigated the roles of the EBPs EatR (regulator of ethanolamine catabolism), DdaR (regulator of methylarginine catabolism), and MifR (regulator of α-ketoglutarate or α-KG transport) in the virulence of *P. aeruginosa* PAO1 in a pneumonia-induced septic mouse model. Deletion of genes encoding EatR and DdaR had no significant effect on the mortality of *P. aeruginosa* PAO1-infected mice compared to wide-type (WT) PAO1-infected mice. In contrast, infected mice with Δ*mifR* mutant exhibited a significant reduction (~50%) in the mortality rate compared with WT PAO1 ($P < 0.05$). Infected mice with Δ*mifR* PAO1 had lower lung injury scores, fewer inflammatory cells, decreased proinflammatory cytokines, and decreased apoptosis and cell death compared to mice infected with WT PAO1 ($P < 0.05$). Furthermore, molecular analysis revealed decreased NLRP3 inflammasome activation in infected mice with Δ*mifR* PAO1 compared to WT PAO1 ($P < 0.05$). These results suggested that the utilization of α-KG was a contributing factor in *P. aeruginosa*-mediated pneumonia and sepsis and that MifR-associated regulation may be a potential therapeutic target for *P. aeruginosa* infectious disease.

KEYWORDS MifR, *P. aeruginosa*, acute infection, alpha-ketoglutarate, enhancer-binding protein, septic mouse model, virulence factors

The bacterium *Pseudomonas aeruginosa* continues to be one of the more challenging pathogens facing healthcare officials and communities. This opportunistic pathogen is a frequent cause of hospital- and community-acquired pneumonia, as well as a common infectious agent in intensive care units (ICUs). Acute infections are more common in hospitalized patients who use ventilators and those infected with *P. aeruginosa* have a 70% to 80% fatality rate (1).

The metabolic demands of *P. aeruginosa* during an infection must be fulfilled from nutrients available in the eukaryotic-host environment. Intriguingly, *P. aeruginosa* relies on an unusual family of transcriptional regulators called enhancer-binding proteins (EBPs) to coordinate the metabolism of several important amino acids, sugars, dicarboxylates, and other organic molecules that are associated with a eukaryotic-host environment and/or infection. For example, the EBP PhhR regulates the catabolism of phenylalanine and

Editor Igor E. Brodsky, University of Pennsylvania

Address correspondence to Benjamin R. Lundgren, lundgrbe@tcnj.edu, or Guirong Wang, wangg@upstate.edu.

The authors declare no conflict of interest.

Received 29 March 2022
Returned for modification 21 June 2022
Accepted 5 September 2022
Published 20 September 2022

tyrosine (2). Both aromatic amino acids are present in the sputum of individuals suffering from cystic fibrosis (CF). Notably, their catabolism has been shown to promote the biosynthesis of the *Pseudomonas* quinolone signal (PQS), thereby enhancing the QS response and subsequent production of virulence factors (2, 3). Other examples include the EBP GcsR, which regulates the catabolism of the mucin-relevant amino acids glycine and serine (4, 5), and the EBP AauR, an essential regulator in the transport of glutamate and glutamine (6), common proteogenic amino acids that are important amino donors for the cell.

Although the metabolic and/or biological functions have now been defined for the majority of EBPs in *P. aeruginosa*, the roles or significance of these regulatory proteins in the virulence of this pathogen have only been investigated for a few of them (5, 7, 8). Therefore, in the current study, we focused on three EBPs known to be involved in the utilization of metabolites associated with a eukaryotic-host environment and evaluated their contributions to *P. aeruginosa*-induced pneumonia and sepsis in mice. The three EBPs of interest were EatR, DdaR, and MifR of *P. aeruginosa* PAO1. The EBP EatR regulates the catabolism of ethanolamine (9), which is derived from the breakdown of the phospholipid phosphatidylethanolamine. Ethanolamine utilization has been associated with the virulence or host interactions of some human pathogens, such as *Salmonella* Typhimurium and *Listeria monocytogenes* (10). Arginine methylation is a common posttranslational modification of eukaryotic proteins (11, 12). The degradation of eukaryotic proteins releases free methylarginines that can be subsequently consumed by various pathogenic microorganisms (13), including *P. aeruginosa* in which regulation by DdaR is essential (14). The EBP MifR of *P. aeruginosa* regulates the expression of the *PA5530* gene, encoding an α-ketoglutarate (α-KG) transporter (15–17). Interestingly, expression analysis of *P. aeruginosa* in the CF lung or when exposed to human airway epithelial cells revealed that the *PA5530* gene was induced (18, 19), suggesting that α-KG might be a key nutrient for this human pathogen in the host environment. To assess the contributions of the EBPs EatR, DdaR, and MifR in the virulence of *P. aeruginosa*, a mouse model of pneumonia and sepsis were used. Mice were infected with each respective ΔEBP mutant, and the mortality and lung injury of infected mice were measured. Additional *in vitro* cytotoxicity assays with a human airway epithelial cell line were conducted to corroborate the results from the *in vivo* mouse studies.

RESULTS

The Δ*eatR*, Δ*ddaR*, and Δ*mifR* mutants exhibited WT levels of virulence factors. Before testing the virulence of the Δ*eatR*, Δ*ddaR*, and Δ*mifR* mutants in a mouse model of pneumonia and sepsis, we first evaluated the EBP mutants for the production of common virulence factors and/or traits, including motility, protease activity, biofilms, pyocyanin, and pyoverdine. Protease activity (Fig. S1A in Supplemental File 1) and motility (Fig. S1B in Supplemental File 1) of the three EBP mutants were similar to the WT. In addition, all three EBP mutants produced pyoverdine (Fig. S2A in Supplemental File 1), pyocyanin (Fig. S2B in Supplemental File 1), and biofilms (Fig. S2C in Supplemental File 1) to levels identical to that of the WT. Collectively, these findings indicated that deletion of the *eatR*, *ddaR,* or *mifR* gene did not negatively affect the production of the aforementioned virulence factors in *P. aeruginosa* PAO1 when assayed under standard laboratory conditions.

Deletion of the *mifR* gene increased the survival time of mice challenged with *P. aeruginosa*-mediated pneumonia and sepsis. To begin to understand the functional relevance of EBPs in the survival and pathogenesis of *P. aeruginosa* in a host environment, we infected mice with the Δ*eatR*, Δ*ddaR*, and Δ*mifR* mutants, as well as WT *P. aeruginosa* PAO1. As shown in Fig. 1, the survival times of mice infected with the Δ*eatR* and Δ*ddaR* mutants were statistically similar to the survival times of mice infected with WT. At 36 h postinfection, the survival probability for mice infected with WT *P. aeruginosa* PAO1 was 50%. A survival probability of 50% was observed at 42 and 39 h for mice infected with the Δ*eatR* or Δ*ddaR* mutants, respectively, and neither one was statistically different from the WT-infected group. In contrast, the survival

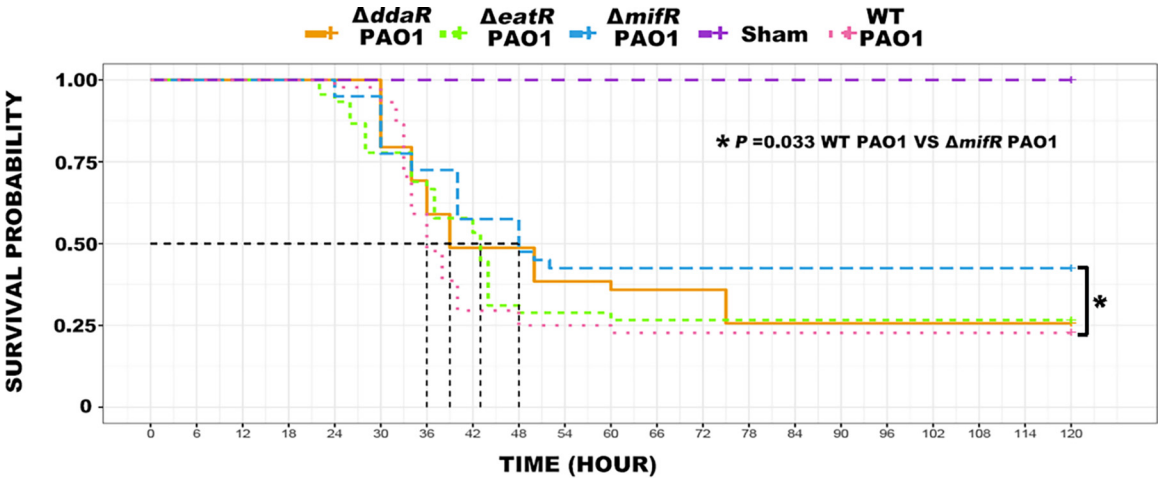

FIG 1 Comparison of the survival time of mice. The animals were treated with wild-type *P. aeruginosa* PAO1 (WT PAO1), Δ*ddaR* PAO1, Δ*eatR* PAO1, Δ*mifR* PAO1 (1×10^6 CFU/mouse), or sterile saline (Sham). The results from the Kaplan-Meier survival analysis showed a lower rate of mortality in the mice infected with Δ*mifR* PAO1 compared with the mice infected with WT PAO1. *, $P = 0.033$, $n = 20$.

probability for mice infected with the Δ*mifR* mutant did not reach 50% until 48 h post-infection. Most deaths of mice infected with the Δ*mifR* mutant occurred after 48 h, whereas those infected with WT *P. aeruginosa* PAO1 were mostly dead before this time. Overall, deletion of a key transcriptional regulator in the utilization of α-KG − but not in the utilization of methylarginines or ethanolamine − increased the survival time of mice when challenged with *P. aeruginosa*-mediated pneumonia and sepsis.

Mice infected with the Δ*mifR* mutant showed reduced lung injury compared to those infected with WT *P. aeruginosa* PAO1. Having established that the *mifR* gene contributed to *P. aeruginosa* PAO1-induced pneumonia and sepsis, we next evaluated the extent of lung injury occurring under such circumstances. It was found that WT *P. aeruginosa* PAO1 caused severe lung damage in mice (Fig. 2). The injured lung showed many inflammatory cells in the alveolar and interstitial space, accumulation of protein fragments, and alveolar septal thickness (Fig. 2A). In comparison, the lungs of mice infected with the Δ*mifR* mutant had a moderate number of inflammatory cells, a small amount of accumulated protein fragments, and only some of the alveolar walls were thickened (Fig. 2B). The lung tissue of the mice in the sham group was normal (Fig. 2C). When the extent of lung injury was scored using a 0 to 2 scale, a mean score of 0.459 was calculated for mice infected with the Δ*mifR* mutant versus a mean score of 0.634 for mice infected with WT *P. aeruginosa* PAO1 (Fig. 2D).

Reduced numbers of inflammatory cells and CFU were observed in the BALF of mice infected with the Δ*mifR* mutant versus WT *P. aeruginosa* PAO1. We compared the total number of macrophages and neutrophils in the bronchoalveolar lavage fluid (BALF) of mice that had either been infected with the Δ*mifR* mutant or WT *P. aeruginosa* PAO1. In both groups, 90% of the observed inflammatory cells in the BALF were neutrophils (Fig. 3A and B). Macrophages were predominantly observed in the BALF of mice in the sham group (Fig. 3C). The total number of alveolar macrophages and neutrophils was significantly lower in the BALF of mice that had been infected with the Δ*mifR* mutant compared to those infected with WT *P. aeruginosa* PAO1 (Fig. 3D and E). In addition, the BALF of mice infected with the Δ*mifR* mutant had a bacterial count of 331.5 CFU ± 129.5 CFU, which was significantly lower than the observed 625.3 CFU ± 252.4 CFU for WT *P. aeruginosa* PAO1 (Fig. 3F).

Mice infected with the Δ*mifR* mutant exhibited decreased levels of plasma cytokines compared to mice infected with WT *P. aeruginosa* PAO1. In a sepsis mouse model induced by pneumonia, the continuous high expression of inflammatory cytokines is an important characteristic (20). Therefore, we measured the levels of three key cytokines, tumor necrosis factor (TNF)-α (Fig. 4A), interleukin (IL)-6 (Fig. 4B), and IL-

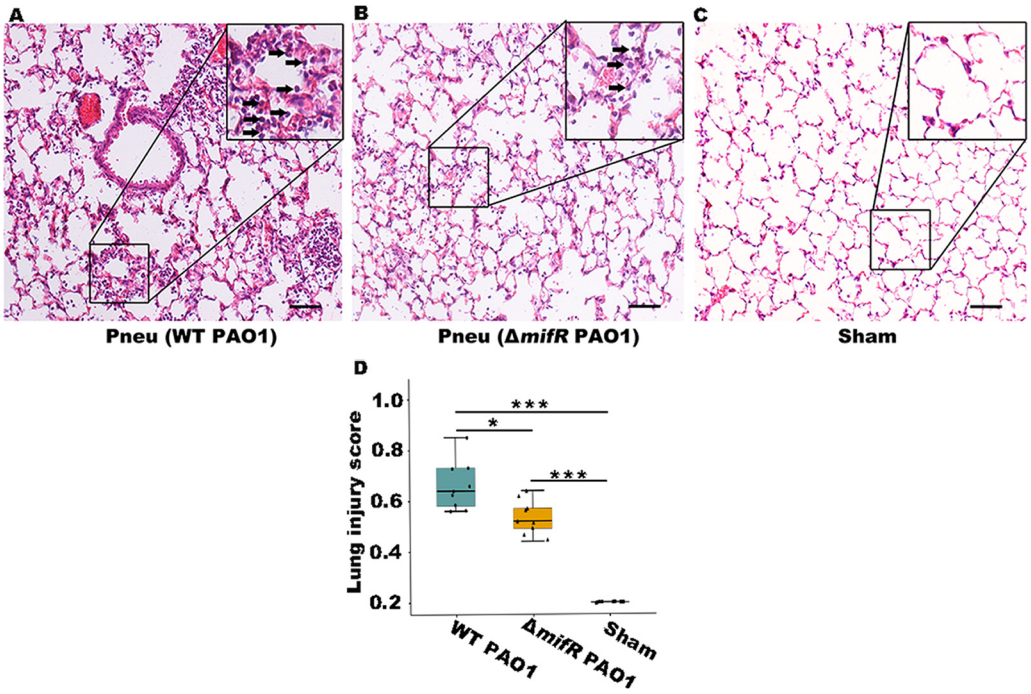

FIG 2 Lung histological examination after infection. Sections of lungs stained with hematoxylin-eosin after infection 24 h are shown for mice infected with (A) WT PAO1, (B) Δ*mifR* PAO1, and (C) Sham group. The lung tissues of the mice of WT PAO1 group (A) showed severe tissue injury, evidenced by large amounts of inflammation cells (black arrows) filled in alveolar spaces and interstitials, proteinaceous debris accumulation, and alveolar septal thickness. (D) Quantitative analysis of lung injury scores indicated that the mice in the Δ*mifR* PAO1 group showed a significantly lower score of lung injury than the mice in the WT PAO1 group. Data points represent mean values ± 25% quantile (box plot) and the minimum and largest observed values (lower and upper edge). $n = 6$; *, $P < 0.05$; ***, $P < 0.001$. Magnification 200×, scale bar = 100 μm. Pneu, pneumonia.

1β (Fig. 4C), in the plasma of mice that had been infected with the Δ*mifR* mutant or WT *P. aeruginosa* PAO1. The mean levels of TNF-α, IL-6, and IL-1β in the plasma of mice infected with WT were 56.1 ±10.7, 484.4 ± 84.1, and 579.4 ± 96.0, respectively (Fig. 4A to C). These levels were significantly greater than those observed in the plasma of mice infected with the Δ*mifR* mutant, which were 37.3 ± 10.5 for TNF-α, 330.8 ± 81.5 for IL-6, and 345.5 ± 82.6 for IL-1β. The measured cytokine levels from the Δ*mifR*-infected mice, however, were still higher than those of the sham group. Furthermore, we also analyzed these three proinflammatory cytokine levels in the BALF (Fig. 4D to F). A similar tendency of these cytokines was observed in this study, i.e., the BALF from WT PAO1-infected mice contained higher levels of TNF-α, IL-6, and IL-1β compared to those from Δ*mifR* mutant-infected mice. The reduced levels of TNF-α, IL-6, and IL-1β in the Δ*mifR*-infected mice indicated that disruption of α-KG transport could lessen the symptoms of systemic inflammatory response syndrome in the early stage of *P. aeruginosa*-mediated pneumonia and sepsis.

Damage and cell death were reduced in the lungs of mice infected with the Δ*mifR* mutant compared to mice infected with WT *P. aeruginosa* PAO1. We investigated the expression of the apoptosis-related protein Bcl-2 and cleaved caspase-3 in the lungs of mice that had been infected with the Δ*mifR* mutant or WT *P. aeruginosa* PAO1 (Fig. 5A). Bcl-2 and cleaved caspase-3 are inhibitors and activators of apoptosis, respectively. Western blotting showed that the levels of Bcl-2 in the lung tissue of mice infected with WT *P. aeruginosa* PAO1 were 35% lower than mice infected with the Δ*mifR* mutant (Fig. 5B). The opposite was observed for levels of cleaved caspase-3 (Fig. 5C). Furthermore, apoptotic cells in the lungs were examined by terminal deoxynucleotidyl transferase dUTP nick end labeling (TUNEL) assay (Fig. 5D to F). The quantitative analysis of apoptotic cells in the lung tissues indicated that there are more apoptotic cells in the lungs from WT PAO1-infected mice compared to Δ*mifR* mutant-infected

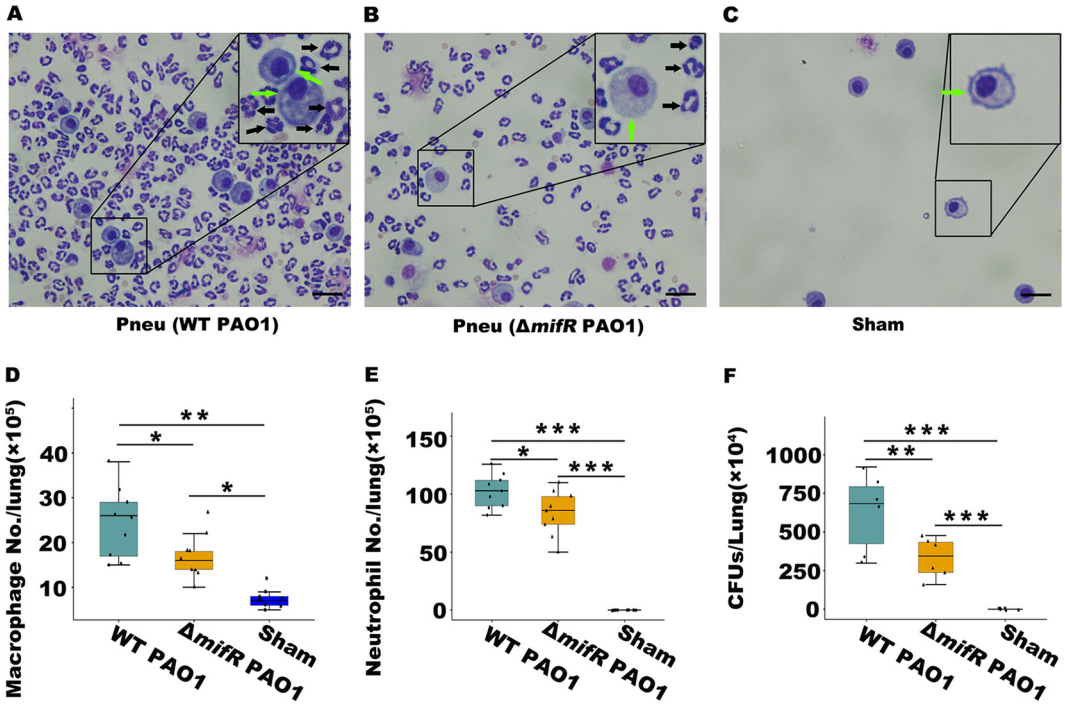

FIG 3 Inflammatory cells and bacteria in BALF from infected mice. Representative images show macrophages and neutrophils in BALF from mice infected with (A)WT PAO1, (B) Δ*mifR* PAO1, and (C) Sham. The cells from BALF are mounted on slides by the cytospin centrifugation and then stained with a HEMA3 staining kit. The results showed that the (C) Sham group of mice only had macrophages (green arrows), and the (A) WT PAO1 and (B) Δ*mifR* PAO1 groups of mice contained more than 90% of neutrophils (black arrows). The measured cell counts of (D) macrophages and (E) neutrophils were significantly lower in the BALF from the Δ*mifR* PAO1 group of mice compared to the WT PAO1 group of mice. (F) Reduced bacteria was observed from the BALF of the Δ*mifR* PAO1 group of mice compared with the WT PAO1 group of mice. Data points represent mean values ± 25% quantile (box plot) and the minimum and largest observed values (lower and upper edge). $n = 6$; *, $P < 0.05$; **, $P < 0.01$; ***, $P < 0.001$. Magnification 400×, scale bar = 50 μm. BALF, bronchoalveolar lavage fluid; Pneu, pneumonia.

mice (Fig. 5G). Collectively, these findings indicated that deletion of the *mifR* gene of *P. aeruginosa* PAO1 weakened its ability to cause cell death during acute lung injury.

We next measured the expression of NLRP3 (an indicator of inflammation), as well as the proteins apoptosis-associated speck-like protein containing a caspase recruitment domain (ASC) and gasdermin D (GSDMD), both of which are related to apoptosis and pyroptosis (Fig. 6A). At 24 h postinfection, the expression levels of NLRP3 (Fig. 6B), ASC (Fig. 6C), and GSDMD (Fig. 6D) in mice infected with WT *P. aeruginosa* PAO1 were significantly higher than those measured in mice that had been infected with the Δ*mifR* mutant. The expression levels of NLRP3, ASC, and GSDMD in the lung tissue of Δ*mifR*-infected mice were still greater than that of the sham group.

Finally, immunofluorescence was used to evaluate the differences in the activation of the NLRP3 inflammasome in the lung tissues of mice infected with WT *P. aeruginosa* PAO1 (Fig. 7A), the Δ*mifR* mutant (Fig. 7B) or the sham group (Fig. 7C). Expression of NLRP3 was activated in mice infected with the WT *P. aeruginosa* PAO1 (Fig. 7A) and to a lesser extent in the Δ*mifR* mutant (Fig. 7B). The NLRP3 inflammasome was not activated in the sham group (Fig. 7C). Notably, there was ~2-fold greater number of NLRP3-positive cells in the lung tissues of mice infected with WT *P. aeruginosa* PAO1 versus those infected with the Δ*mifR* mutant (Fig. 7D).

The Δ*mifR* and Δ*PA5530* mutants displayed decreased cytotoxicity compared to WT *P. aeruginosa* PAO1. The results of our animal study demonstrated that the *mifR* gene was required for the full virulence of *P. aeruginosa* PAO1. The EBP MifR has not been shown to directly regulate the expression of any known virulence factors (15). Instead, in response to extracellular C_5-dicarboxylates, such as α-KG, MifR activates expression of the *PA5530* gene, which encodes for a dicarboxylate-transport protein

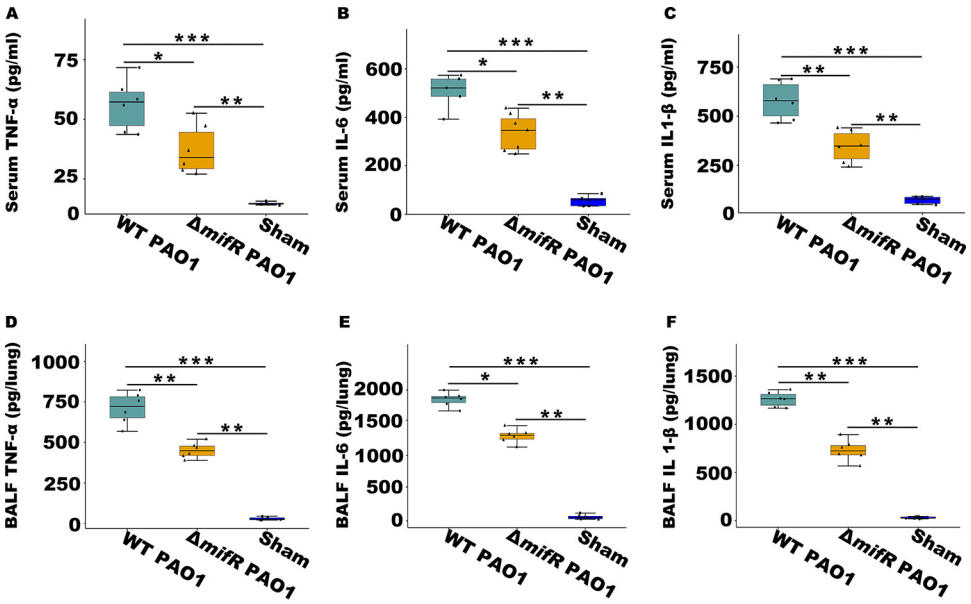

FIG 4 Analysis of cytokines in the serum and lung BALF of mice infected with wild-type *P. aeruginosa* PAO1 (WT PAO1), Δ*mifR* PAO1, or Sham. Serum inflammatory cytokines (A) TNF-α, (B) IL-6, and (C) IL-1β levels were measured in mice infected with WT PAO1, Δ*mifR* PAO1, or Sham via ELISA. The levels of serum TNF-α, IL-6, and IL-1β in mice infected with Δ*mifR* PAO1 were significantly lower than those measured in mice infected with WT PAO1. BALF inflammatory cytokines (D) TNF-α, (E) IL-6, and (F) IL-1β levels showed similar changes in this study. Data points represent mean values ± 25% quantile (box plot) and the minimum and largest observed values (lower and upper edge). $n = 6$; *, $P < 0.05$; **, $P < 0.01$; ***, $P < 0.001$. Magnification 200×, scale bar = 100 μm.

(15, 17). Because MifR and its target *PA5530* gene were essential for the utilization of α-KG in *P. aeruginosa*, it was speculated that *PA5530* might also be necessary for the full virulence of this human pathogen. This was briefly addressed by measuring the cytotoxicity of both Δ*mifR* and Δ*PA5530* mutants towards A549 epithelial cells (Fig. 8). Specifically, the amount of released cytoplasmic lactate dehydrogenase (LDH) from the A549 cells when challenged with the bacteria was used as a measure for cytotoxicity. As shown in Fig. 8A, at 6 h post addition of bacteria, levels of released cytoplasmic LDH were ~50% greater for A549 cells challenged with the WT strain compared to those challenged with the Δ*mifR* and Δ*PA5530* mutants. The cytotoxicity of the Δ*mifR* and Δ*PA5530* mutants was, therefore, lower than that of WT (Fig. 8B). Indeed, a significantly greater percentage of live A549 cells was observed for both the Δ*mifR* and Δ*PA5530* treatments compared to that of WT (Fig. 8C).

To confirm that the reduced cytotoxicity of the Δ*mifR* and Δ*PA5530* mutants was a result of their respective mutations, genetic complementation experiments were conducted. The Δ*mifR* and Δ*PA5530* mutants were transformed with the expression plasmids pJRH08 and pBRL479, which carried the *mifR* and *PA5530* gene, respectively (15). Mutants and WT *P. aeruginosa* PAO1 harboring empty expression plasmid (pBBR1MCS-5) served as controls. Genetic complementation was initially evaluated by growing the recombinant strains in minimal media in which either glucose or α-KG served as the sole carbon source. In the presence of glucose as the sole carbon source, the final cell densities of all recombinant strains were similar, i.e., optical density at 600 nm (OD_{600}) of ~ 1.8 (Fig. 9A). This was not the case when α-KG was the only available carbon source. As shown in Fig. 9A, the Δ*mifR* and Δ*PA5530* mutants harboring empty pBBR1MCS-5 did not grow in a minimal medium with α-KG as the sole carbon source. Both recombinant strains yielded final OD_{600} values <0.1 compared to the OD_{600} of ~0.8 observed for the WT cells carrying pBBR1MCS-5. The growth of the Δ*mifR* and Δ*PA5530* mutants on α-KG was restored to wild-type levels when the *PA5530* gene was expressed from the *lac* promoter of

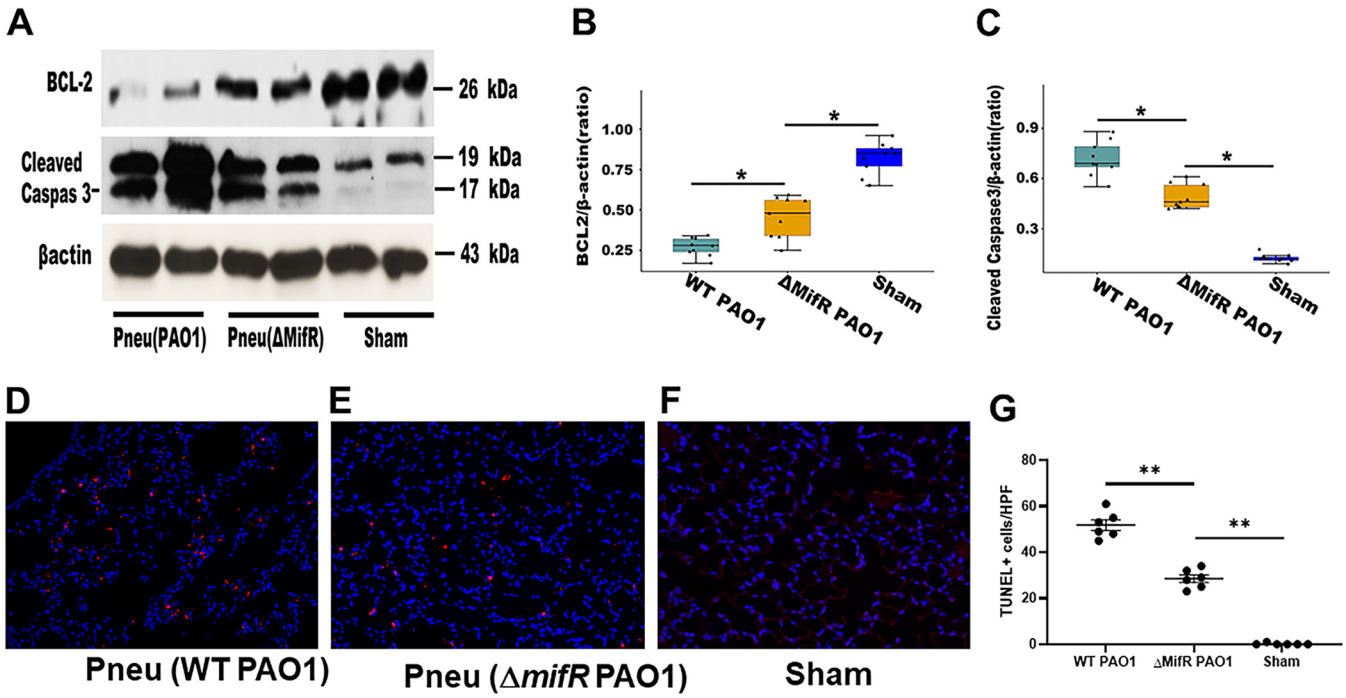

FIG 5 Apoptosis in mice infected with wild-type *P. aeruginosa* PAO1 (WT PAO1), Δ*mifR* PAO1, or Sham. (A) Representative Western blots for Bcl-2 and cleaved caspase-3, (B) quantification of Bcl-2 expression, and (C) quantification of cleaved caspase-3 expression. The levels of apoptosis-related protein are decreased in the Δ*mifR* PAO1 group compared to the WT PAO1 group. Representative images showed TUNEL assay in the lung of mice infected with (D) wild-type *P. aeruginosa* PAO1 (WT PAO1), (E) Δ*mifR* PAO1, or (F) Sham. (G) The quantitative analysis of apoptotic cells in each HPF demonstrated fewer apoptotic cells in the lung of the Δ*mifR* PAO1 group compared to the WT PAO1 group. Data points represent mean values ± 25% quantile (box plot) and the minimum and largest observed values (lower and upper edge). $n = 6$; *, $P < 0.05$; **, $P < 0.01$. Pneu, pneumonia.

pBBR1MCS-5 (Fig. 9A). Expression of *mifR* from pBBR1MCS-5 not only rescued the growth of the Δ*mifR* mutant but enhanced its growth on this dicarboxylate by ~2-fold, resulting in a final OD_{600} of 1.5 (Fig. 9A). Expression of *mifR* from pBBR1MCS-5 did not recover the growth of the Δ*PA5530* mutant on α-KG (Fig. 9A). These results demonstrated successful genetic complementation of the Δ*mifR* and Δ*PA5530* mutants regarding α-KG utilization. Notably, they highlighted the essential nature of these genes in the consumption of this preferred dicarboxylate in *P. aeruginosa*.

We next evaluated the genetic complementation of the Δ*mifR* and Δ*PA5530* mutants as it pertained to cytotoxicity or virulence. As shown in Fig. 9B, reduced cytotoxicity (~30% decrease) towards A549 cells was observed for Δ*mifR* and Δ*PA5530* mutants harboring empty pBBR1MCS-5. In contrast, wild-type levels of cytotoxicity were observed for Δ*mifR* cells expressing *mifR* or *PA5530* from pBBR1MCS-5, whereas full cytotoxicity of the Δ*PA5530* mutant was only restored through expression of *PA5530* and not *mifR* (Fig. 9B). These findings suggested that the reduced virulence of the Δ*mifR* and Δ*PA5530* mutants was a direct result of deletions in the *mifR* and *PA5530* genes, respectively, and not from indirect or secondary effects/mutations.

DISCUSSION

The EBP MifR contributed to the virulence of *P. aeruginosa* PAO1 in a mouse model of pneumonia and sepsis. The *mifR* gene of *P. aeruginosa* PAO1 was required for full virulence in a mouse model of pneumonia and sepsis. It was also necessary for complete cytotoxicity *in vitro*. The EBP MifR is a response regulator that forms a two-component signal transduction system (TCS) with the histidine kinase MifS (15–17). The MifSR TCS detects or senses extracellular C_5-dicarboxylates, such as glutarate and α-KG, and in response, activates transcription of the *PA5530* gene encoding a dicarboxylate-transport protein (15). Notably, micromolar concentrations of α-KG are sufficient to activate the expression of *PA5530* in *P. aeruginosa* PAO1 (15). The MifSR TCS is

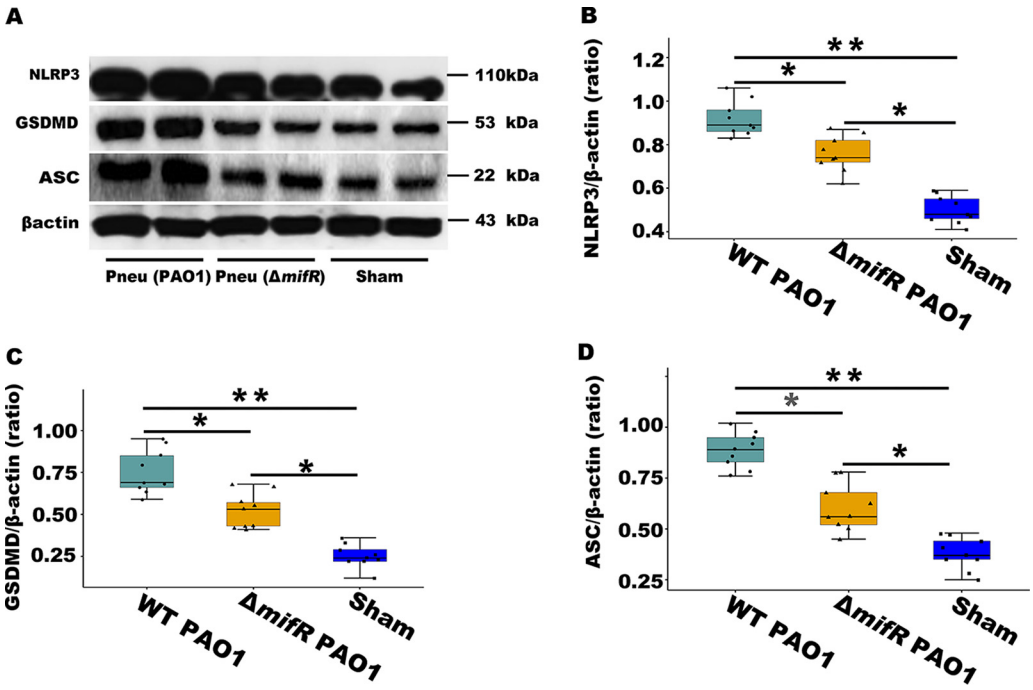

FIG 6 NLRP3 pathway and pyroptosis in mice infected wild-type *P. aeruginosa* PAO1 (WT PAO1), Δ*mifR* PAO1, or Sham. (A) Representative Western blots for NLRP3, GSDMD, and ASC, (B) quantification of NLRP3 expression, (C) quantification of GSDMD expression, and (D) quantification of ASC expression. Data points represent mean values ± 25% quantile (box plot) and the minimum and largest observed values (lower and upper edge). $n = 6$; *, $P < 0.05$; **, $P < 0.01$. Pneu, pneumonia.

specific towards C_5-dicarboxylates, meaning that other organic acids and/or dicarboxylates are not acceptable substrates for the induction of *PA5530* via MifSR (15, 17). Both the MifSR TCS and its target *PA5530* gene are essential for the utilization of α-KG in *P. aeruginosa* PAO1. α-KG and other TCA intermediates are preferred carbon sources for this pathogen. Apart from *PA5530*, no other genes, including those encoding virulence factors or proteins involved in α-KG metabolism, have been experimentally shown to be directly regulated by MifSR TCS. Similarly, to this date, no other transcriptional regulator(s) have been found to directly regulate the expression of *PA5530*.

The reduced virulence of the Δ*mifR* mutant (Fig. 1), as well as the decreased cytotoxicity observed for both the Δ*mifR* and Δ*PA5530* mutants (Fig. 8), is believed to be the direct result of an inability to utilize α-KG from the eukaryotic-host environment. The death or lysis of eukaryotic cells during infection is expected to release α-KG, which is a TCA intermediate, key biosynthetic precursor, and signaling molecule (21). Metabolite profiling of human cell lines revealed that the intracellular concentration of α-KG varied among them, ranging from 70 to 900 μM (22). The release of α-KG to micromolar concentrations in the immediate environment is more than sufficient to induce the expression of *PA5530* via the MifSR TCS in *P. aeruginosa* (15). Indeed, the induction or upregulated transcription of the *PA5530* gene has been previously reported for *P. aeruginosa* when exposed to eukaryotic cells and/or the environment. For example, a microarray study found that following exposure of 4.0 h to human airway epithelial cells, the *PA5530* gene of *P. aeruginosa* PAO1 was induced by >4-fold (18). The induction of *PA5530*, however, was not observed at 12 h postexposure, suggesting that α-KG utilization occurred in the early stages of interaction between *P. aeruginosa* and human airway epithelial cells. In a more recent study, in situ transcriptomics on CF sputum revealed that *PA5530* (or *PA14_72960*) was upregulated in the *P. aeruginosa* population (19). Interestingly, transport of α-KG was observed to be necessary for the virulence of uropathogenic *Escherichia coli* (23). This suggests that

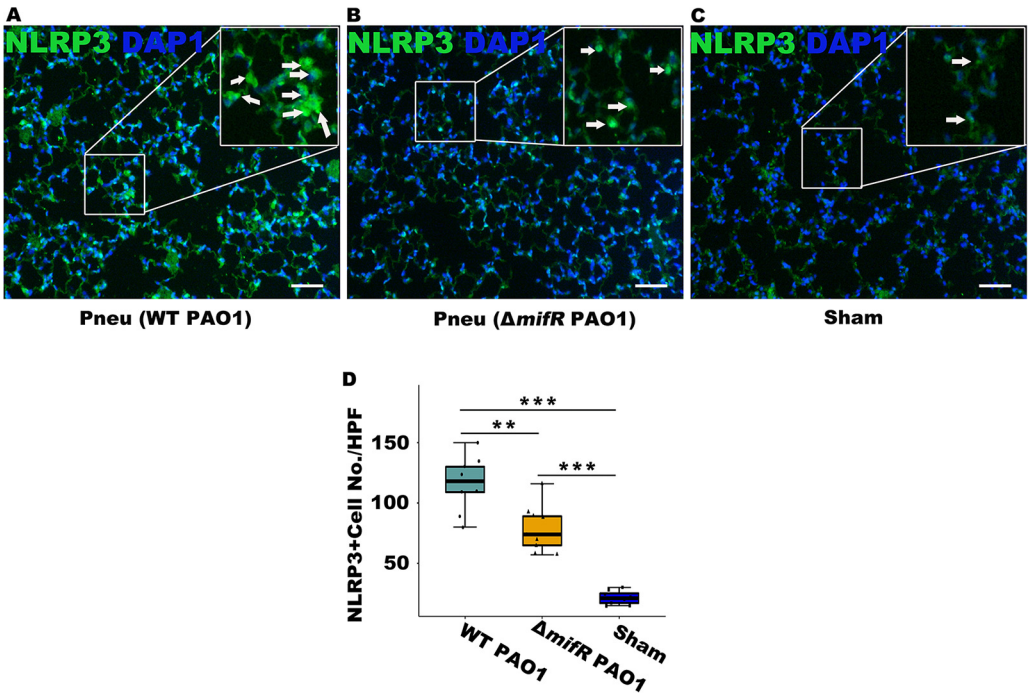

FIG 7 The expression of NLRP3 in immunofluorescence experiment in mice infected with (A) wild-type *P. aeruginosa* PAO1 (WT PAO1), (B) Δ*mifR* PAO1, or (C) Sham. The white arrows in the images indicate the immunofluorescence NLRP3 expression. (D) Statistical analysis of NLRP3 positive cell number was significantly decreased in the mice infected with Δ*mifR* PAO1 compared with the mice infected with WT PAO1. Data points represent mean values ± 25% quantile (box plot) and the minimum and largest observed values (lower and upper edge). $n = 6$; **, $P < 0.01$; ***, $P < 0.001$. Magnification 200×, scale bar = 100 μm. Pneu, pneumonia; HPF, high power field.

the utilization of α-KG may have a broader, more influential role in the virulence of human pathogens than previously thought.

Despite the transcriptomic data surrounding *PA5530*, the presence of α-KG has not been detected in CF sputum (3). The MifSR TCS and its target *PA5530* gene allow *P. aeruginosa* to readily consume extracellular α-KG at concentrations as low as 20 μM (15). Thus, the failure to detect α-KG in CF sputum could be a consequence of the rapid transport/metabolism of this dicarboxylate by *P. aeruginosa*. Although not detected in CF sputum, α-KG was observed in BALF from both healthy individuals and those suffering from acute respiratory distress syndrome (ARDS) (24). Notably, the mean concentration of α-KG in the BALF of patients suffering from ARDS was significantly greater (>8-fold) than that measured for the healthy group. Metabolomic studies aimed at measuring the levels of extracellular α-KG when *P. aeruginosa* is exposed to eukaryotic cells are warranted.

It should be noted that the Δ*mifR* mutant used in this study was indistinguishable from its parental PAO1 strain regarding motility, protease activity, biofilm formation, and the production of pyoverdine and pyocyanin (Fig. S1 and S2 in Supplemental File 1). The reduced virulence observed for the Δ*mifR* mutant, therefore, cannot be attributed to a general (nonspecific) defect in the production of any of these tested virulence factors. In addition, pyocyanin biosynthesis is strictly dependent on PQS and QS (25–27), so the WT levels of pyocyanin produced by the Δ*mifR* mutant is an indicator that neither of these signaling systems is disrupted in its background. Nonetheless, a more detailed investigation into the molecular mechanisms surrounding α-KG utilization in the lung or eukaryotic-cell environment is needed to confirm this hypothesis. Defining the roles of the histidine kinase MifS and the dicarboxylate-transporter PA5530 in the virulence of *P. aeruginosa* is a goal of future work.

The role of EatR, DdaR, and other EBPs in the virulence of *P. aeruginosa*. Unlike MifR, the EBPs EatR and DdaR were not required for the virulence of *P. aeruginosa* PAO1 in a mouse model of pneumonia and sepsis (Fig. 1). The EBP EatR positively regulates the

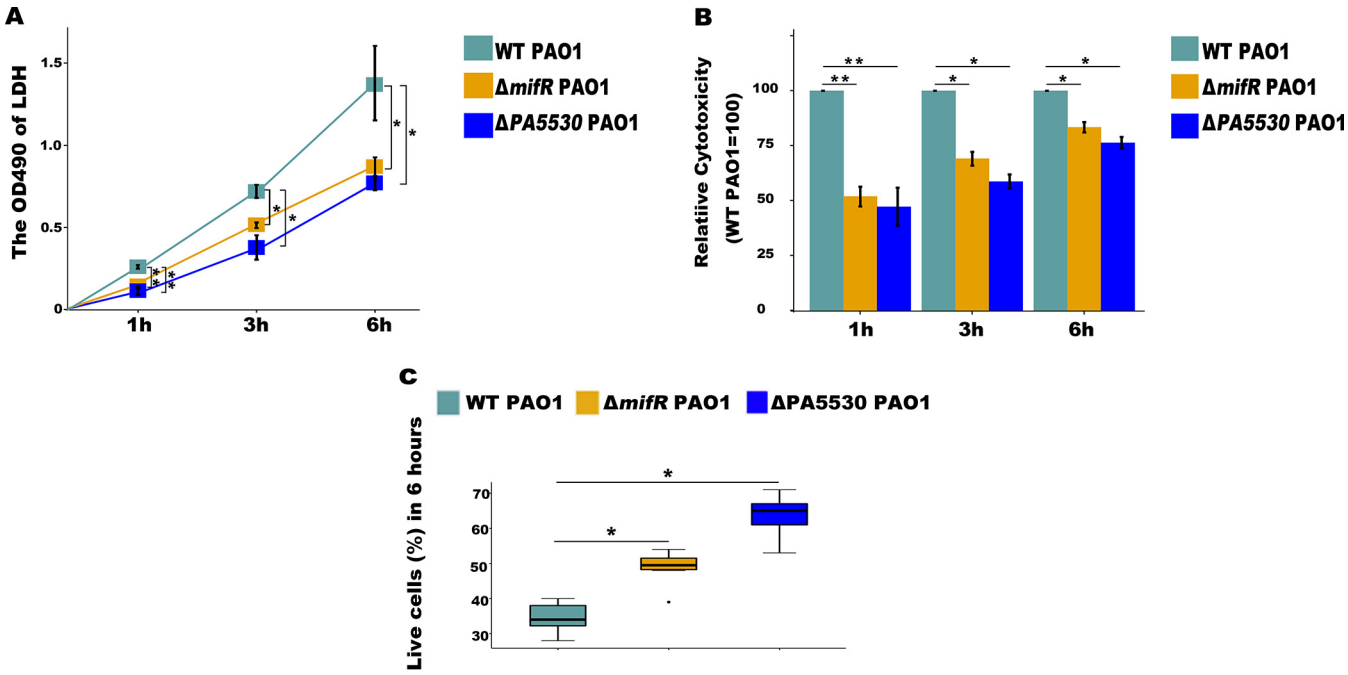

FIG 8 Cytotoxicity of wild-type *P. aeruginosa* PAO (WT PAO1), Δ*mifR* PAO1, and Δ*PA5530* PAO1 on A549 lung epithelial cells. (A) The trends or changes in LDH activity post addition of bacteria. (B) The percentage of LDH secreted by the three different strains at 6 h post addition of bacteria. Levels of LDH secreted by WT were taken as 100%. (C) The percentage of active A549 cells remaining at 6 h post addition of bacteria. Data points represent mean values ± SEM for (A and B), mean values ± 25% quantile (box plot), and the minimum and largest observed values (lower and upper edge) for (C). $n = 3$; *, $P < 0.05$; **, $P < 0.01$. SEM, standard error of the mean.

expression of the *PA4022-eat-eutBC* operon, encoding proteins that are essential in the catabolism of ethanolamine (9). Some data suggests that the animal intestine is a rich source of ethanolamine, both in its free form as well as being bound in the phospholipid phosphatidylethanolamine (10, 28). This might explain why the virulence of some intestinal human pathogens is affected by ethanolamine catabolism (10) while the virulence of *P. aeruginosa* PAO1 in acute lung injury is not.

Our findings also suggested that the catabolism of methylarginines regulated via DdaR was not crucial for the virulence of *P. aeruginosa* PAO1 in acute lung injury. Eukaryotic proteins are the only known major source of methylarginines, and interestingly, several pathogenic microorganisms possess enzymes called dimethylarginine dimethylaminohydrolases that hydrolyze methylarginines to yield citrulline and methylated amines as products (13). For *P. aeruginosa*, the liberated citrulline is a source of nitrogen and ATP (14). Neither citrulline nor methylated amines are a suitable carbon source for *P. aeruginosa*. The limited nutritional value of methylarginines might, therefore, account for the dispensable nature of DdaR in the virulence of *P. aeruginosa* PAO1. In other words, the more preferable nitrogen- and ATP-yielding substrates are available for *P. aeruginosa* during acute lung injury, thereby rendering methylarginine catabolism a nonlimiting factor.

There is a total of twenty-two EBPs encoded in the genome of *P. aeruginosa* PAO1 (29). The biological functions of twenty of the EBPs have either been experimentally described or strongly predicted (2, 4, 6, 9, 14, 15, 29–38). Some of these EBPs directly regulate pathogenic traits, such as motility, alginate, and type IV secretion systems (30, 33, 36, 38). However, the primary functions for thirteen of these EBPs are directed towards the metabolism of *P. aeruginosa*. The EBPs CbrB and NtrC serve as master regulators for the assimilation of carbon and nitrogen, respectively, so one might expect that deletion of either one would negatively impact the virulence of *P. aeruginosa*. While this is true for an Δ*ntrC* mutant (8), transposon mutation of *cbrB* did not affect the virulence of *P. aeruginosa* PA14 in a mouse model (7). Deletion of the *cbrB* gene in *P. aeruginosa* PAO1 did reduce its growth rate in synthetic CF sputum, but its final cell densities were comparable to that of wild-type cells (39).

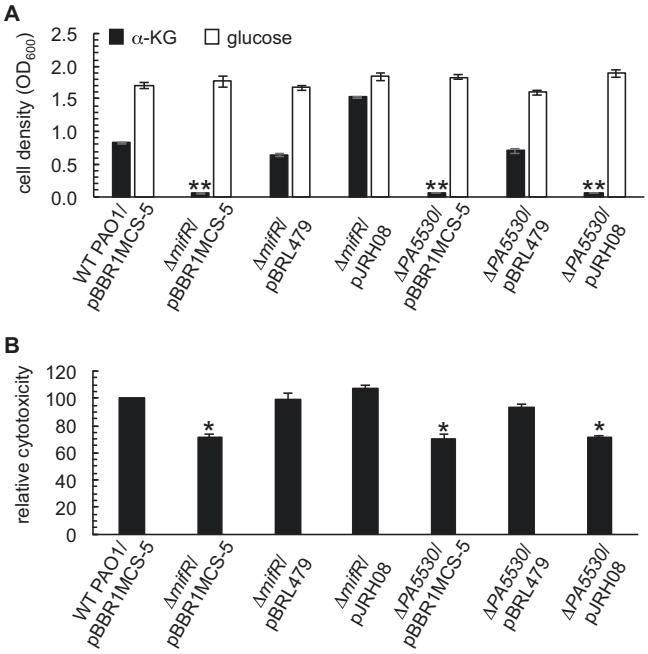

FIG 9 Plasmid-based expression of either the *mifR* or *PA5530* gene in the Δ*mifR* mutant restored its growth on α-KG as the sole carbon source and cytotoxicity towards A549 lung epithelial cells. The Δ*mifR* and Δ*PA5530* mutants of *P. aeruginosa* PAO1 were transformed with expression plasmids carrying no insert (pBBR1MCS-5), *mifR* (pJRH08), or *PA5530* (pBRL479). Wild-type *P. aeruginosa* PAO1 (WT PAO1) carrying pBBR1MCS-5 served as the positive control. Recombinant strains were (A) grown in minimal media in which glucose or α-KG served as the sole carbon source or (B) tested for relatively cytotoxicity towards A549 lung epithelial cells in which WT PAO1/pBBR1MCS-5 was equated to 100. As expected, wild-type levels of growth on α-KG and cytotoxicity were observed for the Δ*mifR* mutant carrying pJRH08 or pBRL479 but not empty pBBR1MCS-5. Recovery of growth on α-KG and cytotoxicity was only observed for the Δ*PA5530* mutant harboring pBRL479. Data points represent mean values ± SEM. $n = 3$; *, $P < 0.05$; **, $P < 0.01$. SEM, standard error of the mean.

Of the remaining eleven EBPs associated with the metabolism of *P. aeruginosa*, only four of them have been investigated in terms of virulence. This includes the three described in the current study, EatR, DdaR, and MifR. The fourth one, GcsR, responds to intracellular glycine and activates the transcription of a glycine-cleavage system that aids in the metabolism of both glycine and serine (4, 5). Glycine is a key component of mucin and serves as a precursor in the biosynthesis of hydrogen cyanide in *P. aeruginosa* (40, 41). When *C. elegans* was challenged with a Δ*gcsR* mutant, the survival time of this worm decreased by >60% compared to those challenged with the parental PAO1 strain (5). The enhanced killing observed for the Δ*gcsR* mutant was hypothesized to be the result of elevated levels of hydrogen cyanide generated from the intracellular pool of nonmetabolized glycine.

Lastly, EBPs involved in the metabolism of *P. aeruginosa* that have not been investigated regarding its virulence include the C_4-dicarboxylate-transport regulator DctD, the glutamate-transport regulator AauR and the aromatic-amino acid catabolism regulator PhhR (2, 6, 35). These EBPs are vital for the utilization of these compounds, which have been detected in CF sputum and/or human airway fluids (24, 42). The EBP AcoR is predicted to regulate the catabolism of acetoin while the EBPs SfnR1 and SfnR2 regulate the catabolism of dimethylsulfide (29, 37). Some data suggests that acetoin might be an important interspecies metabolite between *Staphylococcus aureus* and *P. aeruginosa*, whereas dimethylsulfide produced by *P. aeruginosa* serves as a sulfur source for the fungal pathogen *Aspergillus fumigatus* (43, 44). Both *S. aureus* and *Aspergillus fumigatus* are frequently isolated as copathogens in *P. aeruginosa*-related infections in cystic fibrosis (45, 46). Whether the EBPs AcoR, SfnR1, and SfnR2 are crucial for such interactions in the diseased state is under investigation.

MATERIALS AND METHODS

Bacterial strain and mutants. Bacteria used in the study consisted of wild-type (WT) *P. aeruginosa* PAO1 and the isogenic mutants Δ*eatR*, Δ*ddaR*, Δ*mifR*, and Δ*PA5530* (9, 14, 15, 47). The bacteria were grown at 37°C in Luria-Bertani broth (LB) or on a solid medium comprised of LB-agar. Peptone broth and Kings B medium were used for assaying the production of pyocyanin and pyoverdine, respectively, and were prepared as previously described (48).

Analysis of virulence factors. All analyses were done in triplicate ($n = 3$) for each strain. For assessing motility, single colonies of each strain or mutant were stabbed into motility test agar plates (Neogen), which were then incubated at 25°C for 48 h. Protease activity was examined by growing each strain or mutant on skim milk agar (HiMedia) at 25°C for 48 h. To evaluate the production of pyocyanin or pyoverdine, bacteria were first grown in 2.0 mL of LB in a 16 × 125 mm culture tube at 37°C at 200 rpm for 18 h. The LB-grown seed cultures were used at 1% (v/v), i.e., 20 μL, to inoculate 2.0 mL of peptone broth (pyocyanin production) or Kings B medium (pyoverdine production) in a 16 × 125 mm culture tube, and the inoculated cultures were grown at 37°C at 200 rpm for 18 h. Cells were removed via centrifugation and subsequent passage through a 0.2 μm syringe filter. The absorbance at 690 or 405 nm was measured for the cell-free supernatants to determine the relative levels of pyocyanin and pyoverdine, respectively (48). For assessing biofilm formation, LB-grown seed cultures of the bacteria were used at 1% (v/v) to inoculate fresh LB. The inoculated LB cultures were aliquoted (100 μL) into a 96-well flat bottom polystyrene microplate (BD Falcon) that was subsequently incubated at 25°C for 48 h. Staining and quantification of the biofilms were done exactly as described (49).

Cytotoxicity assays. Cytotoxicity assays were conducted in triplicate ($n = 3$) for each strain or mutant. Single colonies were inoculated in 5.0 mL of LB and incubated at 37°C at 250 rpm for 18 h. Bacteria were collected via centrifugation and subsequently diluted in MEM to yield ~ 4.0×10^7 CFU mL^{-1}. These bacterial suspensions served as the inocula for the cytotoxicity assays.

The human lung adenocarcinoma epithelial cell line A549 was purchased from ATCC (no. CCL-185) and was cultured in 6-well plates in minimal essential medium (MEM) supplemented with 10% (v/v) fetal bovine serum and 1% (w/v) L-glutamine (Gibco by Life Technologies, Thermo Fisher Scientifc, USA). When the number of A549 cells in the 6-well plate reached ~90% of the plate area, they were treated with 3 mL of the bacterial suspensions. The bacterial-treated A549 cells were grown at 37°C and 5% CO_2 (the multiplicity of infection [MOI] at this time was 20). At 1.0, 3.0, and 6.0 h after the addition of bacteria, 50 μL of the medium from bacterial-treated A549 culture was collected for the analysis of LDH activity according to the protocol of Cytotox 96 nonradioactive cytotoxicity kit (Promega, lot no. 0000461938). Cytotoxicity percentage was equal to experimental LDH release (OD490)/maximum LDH release (OD_{490}) (50). In addition, the percentage of viable cells was counted with a cell counter.

Genetic complementation experiments. The *mifR* and *PA5530* genes were previously cloned under the *lac* promoter of the broad-host-range plasmid pBBR1MCS-5 to yield pJRH08 and pBRL479, respectively (15). The pJRH08, pBRL479, and empty pBBR1MCS-5 plasmids were introduced into the Δ*mifR* and Δ*PA5530* mutants via electroporation (15), and wild-type *P. aeruginosa* PAO1 carrying pBBR1MCS-5 was used as the positive control. Recombinant strains in triplicate ($n = 3$) were subjected to two sets of genetic complementation experiments. First, using a previously described microplate assay (14), recombinant strains were grown at 37°C with shaking in minimal medium (22 mM KH_2PO_4, 42 mM Na_2HPO_4, 8.6 mM NaCl, 18.7 mM NH_4Cl, 1.0 mM $MgSO_4$, and 5.0 μM $FeSO_4$, pH 7.0) supplemented with 30 mg L^{-1} gentamicin and either 20 mM glucose or α-KG as the sole carbon source (15). At 24 h postinoculation, the absorbance at 600 nm or optical density (OD_{600}) was measured for each bacterial culture. Second, recombinant strains were subjected to cytotoxicity assays performed exactly as described earlier except that the media used for culturing the recombinant strains was supplemented with 30 mg L^{-1} gentamicin.

Mice and maintaining conditions. We used wild-type FVB/N, which was originally purchased from the Jackson Laboratory (Bar Harbor, ME). All mice were kept pathogen-free in the animal core facility at the State University of New York (SUNY) Upstate Medical University with a standard12 h/12 h light/dark time cycle, the stable controlled temperature at 24°C, and regular mice feed and water. Both male and female WT mice (8 to 12 weeks old, ~25 g body weight [bw]) were used for the study (20, 51). Mice were infected with wild-type *P. aeruginosa* PAO1 (WT PAO1), or each *P. aeruginosa* PAO1 mutant (1×10^6 CFU/mouse), and Sham mice were treated with the same volume of saline to replace bacterial solution (52). All relevant animal experiments are in strict compliance with the National Institutes of Health and the Animal Research: Reporting of *In Vivo* Experiments (ARRIVE) guidelines and have been approved by the State University of New York Upstate Medical University Institutional Animal Care and Use Committee (IACUC number 380).

***P. aeruginosa*-induced pneumonia and sepsis model.** This analysis included wild-type *P. aeruginosa* PAO1 and the Δ*eatR*, Δ*ddaR*, and Δ*mifR* mutants. Bacteria were grown in LB at 37°C at 200 rpm to late-log growth at which time 1.0 mL was collected via centrifugation and subsequently suspended in cold, buffered saline to yield an absorbance of 0.6 at 600 nm. The bacteria were diluted an additional 40-fold in buffered saline, and 50 μL of the diluted bacterial suspension was injected into the mouse. The procedures of anesthesia, surgery and intratracheal inoculation of bacteria were performed as described previously (53).

Collection and analysis of mice bronchoalveolar lavage fluid. Mice were anesthetized by intraperitoneal injection of ketamine/thiazide (90 mg kg^{-1} ketamine, 10 mg kg^{-1} thiazide) and then sacrificed by bleeding. A 1.0 mL syringe was used to collect blood from the inferior vena cava of the mouse. The collected blood was centrifuged at 3000 rpm for 10 min, and the supernatant was subjected to an enzyme-linked immunosorbent assay (ELISA; see below). Lung tissue and BALF were collected as previously described (20, 51). To determine the number of bacteria present in the BALF from each mouse, the

collected BALF (100 μL) was diluted 1000-fold, and in triplicate (n = 3),100 μL of this dilution was plated on LB-agar. Following an incubation period of 18 h at 37°C, the CFU was counted, averaged, and reported as total CFU per lung (54). The quantification of inflammatory cells present in mice BALF has been described (51). Briefly, the total number of cells present in each BALF was determined with a hemocytometer. Next, the cells in each BALF were collected by centrifugation, suspended in 1.0 mL of cold buffered saline, and finally mounted to a slide by a cytospin centrifuge (Hettich ROTOFIX32 A) at 1,000 rpm for 3 min. The mounted or fixed slides were stained with HEMA 3 Cell Staining kit (Fischer Scientific catalog no. 122911), and the macrophages/monocytes and polymorphonuclear neutrophils (PMN) were identified and quantified with a Nikon Eclipse TE2000-U research microscope (Nikon, Melville, NY).

Lung histopathological analysis. The lung tissues of the mice were fixed with 10% (w/v) formalin for 24 h and embedded in the paraffin block. About 5-μm sections were stained with hematoxylin and eosin (H&E) as described previously (55). Slides were examined under a Nikon Eclipse TE2000-U research microscope (Nikon, Melville, NY) and digital photographs were taken, acute lung injury was evaluated as described in our previous publication (55).

Terminal deoxynucleotidyl transferase dUTP nick end labeling assay. TUNEL analysis was performed as described in our recent publication (51). In brief, formalin-fixed, paraffin-embedded, 5-μm slides of lung tissue were incubated at 60°C for 1 h, then deparaffinized. Slides were fixed with 4% paraformaldehyde for 15 min and treated with proteinase K for permeabilization. After that, slides were treated and incubated with a Click-iT Plus TUNEL reaction cocktail at 37°C for 30 min. Slides were mounted by fluoroshield mounting medium with DAPI (ab104139, Abcam, Cambridge, MA) to visualize cell nuclei. Apoptotic cells were quantified at each high-power field ($\times$200 magnification) by counting the number of TUNEL-positive cells in 10 randomly chosen fields.

Western blotting. Western blotting was performed as described in our previous publication (55). In brief, frozen lung tissue was homogenized in radioimmunoprecipitation assay (RIPA) buffer containing a mixture of protease and phosphatase inhibitors. The homogenized lung samples were centrifuged, and the resulting supernatants were assayed for total protein via a micro-BCA assay kit (Thermo Scientific, Rockford, IL). Next, each sample (30 μg of total protein) was dissolved by reduction, electrophoresed on a 12% SDS-polyacrylamide gel, and then transferred to a PVDF membrane (Bio-Rad, Hercules, CA, USA). The blot was blocked in Tris-buffered saline/0.1% Tween20 (TBST) containing 5% skim milk for 1.0 h at room temperature to remove the nonspecific binding and subsequently incubated with the primary antibodies listed below at 4°C overnight with shaking. Subsequently, the blot was incubated with an enzyme-labeled secondary antibody (Bio-Rad, Hercules, CA) at room temperature for 1 hour, detected with Pierce ECL Western blotting substrate/detection reagent (Thermo Scientific, Rockford, IL), and exposed with X-ray film (Pierce Biochemicals, FL). Image J software version 1.48 (Wayne Rasband, NIH, Bethesda, MA) was used to scan and quantify the film. The main antibody used for western blotting, ASC (67824s Santa Cruz Biotechnology, Dallas, TX), BCL-2 (3498s Santa Cruz Biotechnology, Dallas, TX), Cleaved caspase-3 (9661s, Santa Cruz Biotechnology, Dallas, TX), NLRP3 (ma5-20838, Thermo Fisher Scientific, Rockford, Illinois), GSDMD (ab209845, Abcam, Cambridge, MA). β-actin antibody (ab16039, Abcam, Cambridge, MA) was used as an internal control. In some experiments, the blot was stripped to remove the antibody, incubated in stripping buffer (Thermo Fisher Scientific, Rockford, IL) at 50°C for 30 minutes, and then tested again with a second primary antibody. Sham mouse lung tissue was used as a positive control.

Cytokine analysis by ELISA. Cytokines were measured by ELISA as described previously (51). Serum and BALF IL-6, IL-1β, and TNF-α levels of three groups of mice were determined using a mouse ELISA kit according to the manufacturer's instructions (Thermo Fisher Scientific, Rockford, IL).

Immunofluorescence analysis. As previously mentioned (20), paraffin-embedded lung sections were performed with immunofluorescence staining. In short, the slides were incubated at 60°C for 1 hour, then deparaffinized with xylene, and then subjected to a graded series of ethanol treatments. The slides were then recovered with citrate buffer antigen (1$\times$, pH 6.0, Sigma-Aldrich, St. Louis, MO) at boiling point for 10 minutes, and then immersed in 0.02% Triton X-100 (T9284, Sigma-Aldrich, MO) at the boiling point), which lasted 45 minutes. After blocking with 10% donkey serum (ab7475, Abcam, Cambridge, MA) for 1 hour at room temperature, the slides were immunostained with the first antibodies listed below at 4°C overnight, and then with donkey anti-rabbit IgG Alexa 488 (ab150073, at room temperature (protected from light), the secondary antibody was conjugated to the secondary antibody for 1 h. DAPI (ab104139, Abcam, Cambridge, MA) slides were used to visualize the nucleus. In a fluorescence microscope (Nikon, the image was viewed and digitized under Melville, NY). The antibody used for immunofluorescence staining was NLRP3 (PA5-20838, Thermo Fisher Scientific, Rockford, IL).

Statistical analysis. SigmaStat Software (version 3.5) was used for statistical analysis. Significant differences between samples and/or groups were determined through one-way analysis of variance (ANOVA) or t test in Fig. 2 to 9. The Kaplan-Meier method was used for analyzing the survival times of infected mice in Fig. 1. For all comparisons, $P < 0.05$ was considered statistically significant.

Ethics statement. All animal experiments and protocols were conducted in accordance with the guidelines of the Institutional Animal Care and Use Committee (IACUC), SUNY Upstate Medical University, those of the National Institutes of Health guidelines on the use of laboratory animals, and those of 'ARRIVE' on the use of laboratory animals.

SUPPLEMENTAL MATERIAL

Supplemental material is available online only.

SUPPLEMENTAL FILE 1, PDF file, 1.5 MB.

ACKNOWLEDGMENTS

This study is supported in part by NIH R01HL136706, and National Science Foundation (NSF) research award (1722630) (to G.W.) and R15GM104880-03 (to B.L.).

All the authors declared no competing interests.

W.X., A.P., I.J., B.L., and G.W. performed experiments, analyzed data, interpreted results, and drafted the manuscript. G.W. and B.L. conceived the study, designed experiments, and wrote the manuscript.

REFERENCES

1. Chastre J, Fagon J-Y. 2002. Ventilator-associated pneumonia. Am J Respir Crit Care Med 165:867–903. https://doi.org/10.1164/ajrccm.165.7.2105078.
2. Palmer GC, Palmer KL, Jorth PA, Whiteley M. 2010. Characterization of the *Pseudomonas aeruginosa* transcriptional response to phenylalanine and tyrosine. J Bacteriol 192:2722–8. https://doi.org/10.1128/JB.00112-10.
3. Palmer KL, Aye LM, Whiteley M. 2007. Nutritional cues control *Pseudomonas aeruginosa* multicellular behavior in cystic fibrosis sputum. J Bacteriol 189:8079–8087. https://doi.org/10.1128/JB.01138-07.
4. Lundgren BR, Thornton W, Dornan MH, Villegas-Peñaranda LR, Boddy CN, Nomura CT. 2013. Gene PA2449 is essential for glycine metabolism and pyocyanin biosynthesis in *Pseudomonas aeruginosa* PAO1. J Bacteriol 195: 2087–100. https://doi.org/10.1128/JB.02205-12.
5. Sarwar Z, Lundgren BR, Grassa MT, Wang MX, Gribble M, Moffat JF, Nomura CT. 2016. GcsR, a TyrR-like enhancer-binding protein, regulates expression of the glycine cleavage system in *Pseudomonas aeruginosa* PAO1. mSphere 1:e00020-16. https://doi.org/10.1128/mSphere.00020-16.
6. Lundgren BR, Shoytush JM, Scheel RA, Sain S, Sarwar Z, Nomura CT. 2021. Utilization of L-glutamate as a preferred or sole nutrient in *Pseudomonas aeruginosa* PAO1 depends on genes encoding for the enhancer-binding protein AauR, the sigma factor RpoN and the transporter complex AatJQMP. BMC Microbiol 21:83. https://doi.org/10.1186/s12866-021-02145-x.
7. Yeung AT, Janot L, Pena OM, Neidig A, Kukavica-Ibrulj I, Hilchie A, Levesque RC, Overhage J, Hancock RE. 2014. Requirement of the *Pseudomonas aeruginosa* CbrA sensor kinase for full virulence in a murine acute lung infection model. Infect Immun 82:1256. https://doi.org/10.1128/IAI.01527-13.
8. Alford MA, Baghela A, Yeung ATY, Pletzer D, Hancock REW. 2020. NtrBC regulates invasiveness and virulence of *Pseudomonas aeruginosa* during high-density infection. Front Microbiol 11:773. https://doi.org/10.3389/fmicb.2020.00773.
9. Lundgren BR, Sarwar Z, Pinto A, Ganley JG, Nomura CT. 2016. Ethanolamine catabolism in *Pseudomonas aeruginosa* PAO1 is regulated by the enhancer-binding protein EatR (PA4021) and the alternative sigma factor RpoN. J Bacteriol 198:2318. https://doi.org/10.1128/JB.00357-16.
10. Kaval KG, Garsin DA. 2018. Ethanolamine utilization in bacteria. mBio 9: e00066-18. https://doi.org/10.1128/mBio.00066-18.
11. Gary JD, Clarke S. 1998. RNA and protein interactions modulated by protein arginine methylation. Prog Nucleic Acid Res Mol Biol 61:65–131. https://doi.org/10.1016/s0079-6603(08)60825-9.
12. Morales Y, Cáceres T, May K, Hevel JM. 2016. Biochemistry and regulation of the protein arginine methyltransferases (PRMTs). Arch Biochem Biophys 590:138–152. https://doi.org/10.1016/j.abb.2015.11.030.
13. Santa Maria J, Vallance P, Charles IG, Leiper JM. 1999. Identification of microbial dimethylarginine dimethylaminohydrolase enzymes. Mol Microbiol 33:1278. https://doi.org/10.1046/j.1365-2958.1999.01580.x.
14. Lundgren BR, Bailey FJ, Moley G, Nomura CT. 2017. DdaR (PA1196) regulates expression of dimethylarginine dimethylaminohydrolase for the metabolism of methylarginines in *Pseudomonas aeruginosa* PAO1. J Bacteriol 199:e00001-17. https://doi.org/10.1128/JB.00001-17.
15. Lundgren BR, Villegas-Peñaranda LR, Harris JR, Mottern AM, Dunn DM, Boddy CN, Nomura CT. 2014. Genetic analysis of the assimilation of C_5-dicarboxylic acids in *Pseudomonas aeruginosa* PAO1. J Bacteriol 196:2543. https://doi.org/10.1128/JB.01615-14.
16. Tatke G, Kumari H, Silva-Herzog E, Ramirez L, Mathee K. 2015. *Pseudomonas aeruginosa* MifS-MifR two-component system is specific for α-ketoglutarate utilization. PLoS One 10: e0129629. https://doi.org/10.1371/journal.pone.0129629.
17. Sarwar Z, Wang MX, Lundgren BR, Nomura CT. 2020. MifS, a DctB family histidine kinase, is a specific regulator of α-ketoglutarate response in *Pseudomonas aeruginosa* PAO1. Microbiology 166:867. https://doi.org/10.1099/mic.0.000943.
18. Frisk A, Schurr JR, Wang G, Bertucci DC, Marrero L, Hwang SH, Hassett DJ, Schurr MJ. 2004. Transcriptome analysis of P*seudomonas aeruginosa* after interaction with human airway epithelial cells. Infect Immun 72:5433. https://doi.org/10.1128/IAI.72.9.5433-5438.2004.
19. Rossi E, Falcone M, Molin S, Johansen HK. 2018. High-resolution in situ transcriptomics of *Pseudomonas aeruginosa* unveils genotype independent patho-phenotypes in cystic fibrosis lungs. Nat Commun 9:3459. https://doi.org/10.1038/s41467-018-05944-5.
20. Yu J, Ni L, Zhang X, Zhang J, Abdel-Razek O, Wang G. 2019. Surfactant protein D dampens lung injury by suppressing NLRP3 inflammasome activation and NF-κB signaling in acute pancreatitis. Shock 51:557. https://doi.org/10.1097/SHK.0000000000001244.
21. Wu N, Yang M, Gaur U, Xu H, Yao Y, Li D. 2016. Alpha-ketoglutarate: physiological functions and applications. Biomol Ther 24:1–8. https://doi.org/10.4062/biomolther.2015.078.
22. Røst LM, Brekke Thorfinnsdottir L, Kumar K, Fuchino K, Eide Langørgen I, Bartosova Z, Kristiansen KA, Bruheim P. 2020. Absolute quantification of the central carbon metabolome in eight commonly applied prokaryotic and eukaryotic model systems. Metabolites 10:74. https://doi.org/10.3390/metabo10020074.
23. Cai W, Cai X, Yang Y, Yan S, Zhang H. 2017. Transcriptional control of dual transporters involved in α-ketoglutarate utilization reveals their distinct roles in uropathogenic *Escherichia coli*. Front Microbiol 8:275. https://doi.org/10.3389/fmicb.2017.00275.
24. Evans CR, Karnovsky A, Kovach MA, Standiford TJ, Burant CF, Stringer KA. 2014. Untargeted LC-MS metabolomics of bronchoalveolar lavage fluid differentiates acute respiratory distress syndrome from health. J Proteome Res 13:640. https://doi.org/10.1021/pr4007624.
25. Whiteley M, Lee KM, Greenberg EP. 1999. Identification of genes controlled by quorum sensing in *Pseudomonas aeruginosa*. Proc Natl Acad Sci U S A 96:13904. https://doi.org/10.1073/pnas.96.24.13904.
26. Chugani SA, Whiteley M, Lee KM, D'Argenio D, Manoil C, Greenberg EP. 2001. QscR, a modulator of quorum-sensing signal synthesis and virulence in *Pseudomonas aeruginosa*. Proc Natl Acad Sci U S A 98:2752. https://doi.org/10.1073/pnas.051624298.
27. Gallagher LA, McKnight SL, Kuznetsova MS, Pesci EC, Manoil C. 2002. Functions required for extracellular quinolone signaling by *Pseudomonas aeruginosa*. J Bacteriol 184:6472–6480. https://doi.org/10.1128/JB.184.23.6472-6480.2002.
28. Bertin Y, Girardeau JP, Chaucheyras-Durand F, Lyan B, Pujos-Guillot E, Harel J, Martin C. 2011. Enterohaemorrhagic *Escherichia coli* gains a competitive advantage by using ethanolamine as a nitrogen source in the bovine intestinal content. Environ Microbiol 13:365–377. https://doi.org/10.1111/j.1462-2920.2010.02334.x.
29. Studholme DJ, Dixon R. 2003. Domain architectures of sigma54-dependent transcriptional activators. J Bacteriol 185:1757–1767. https://doi.org/10.1128/JB.185.6.1757-1767.2003.
30. Wozniak DJ, Ohman DE. 1991. *Pseudomonas aeruginosa* AlgB, a two-component response regulator of the NtrC family, is required for *algD* transcription. J Bacteriol 173:1406–1413. https://doi.org/10.1128/jb.173.4.1406-1413.1991.
31. Ishimoto KS, Lory S. 1992. Identification of *pilR*, which encodes a transcriptional activator of the *Pseudomonas aeruginosa* pilin gene. J Bacteriol 174:3514. https://doi.org/10.1128/jb.174.11.3514-3521.1992.
32. Nishijyo T, Haas D, Itoh Y. 2001. The CbrA-CbrB two-component regulatory system controls the utilization of multiple carbon and nitrogen sources in P*seudomonas aeruginosa*. Mol Microbiol 40:917. https://doi.org/10.1046/j.1365-2958.2001.02435.x.
33. Dasgupta N, Wolfgang MC, Goodman AL, Arora SK, Jyot J, Lory S, Ramphal R. 2003. A four-tiered transcriptional regulatory circuit controls

flagellar biogenesis in *Pseudomonas aeruginosa*. Mol Microbiol 50:809. https://doi.org/10.1046/j.1365-2958.2003.03740.x.
34. Li W, Lu CD. 2007. Regulation of carbon and nitrogen utilization by CbrAB and NtrBC two-component systems in *Pseudomonas aeruginosa*. J Bacteriol 189:5413. https://doi.org/10.1128/JB.00432-07.
35. Valentini M, Storelli N, Lapouge K. 2011. Identification of C(4)-dicarboxylate transport systems in *Pseudomonas aeruginosa* PAO1. J Bacteriol 193:4307. https://doi.org/10.1128/JB.05074-11.
36. Sana TG, Soscia C, Tonglet CM, Garvis S, Bleves S. 2013. Divergent control of two type VI secretion systems by RpoN in *Pseudomonas aeruginosa*. PLoS One 8:e76030. https://doi.org/10.1371/journal.pone.0076030.
37. Lundgren BR, Sarwar Z, Feldman KS, Shoytush JM, Nomura CT. 2019. SfnR2 regulates dimethyl sulfide-related utilization in *Pseudomonas aeruginosa* PAO1. J Bacteriol 201:e00606-18. https://doi.org/10.1128/JB.00606-18.
38. Kilmury SLN, Burrows LL. 2018. The *Pseudomonas aeruginosa* PilSR two-component system regulates both twitching and wwimming motilities. mBio 9:e01310-18. https://doi.org/10.1128/mBio.01310-18.
39. Sonnleitner E, Valentini M, Wenner N, Haichar FZ, Haas D, Lapouge K. 2012. Novel targets of the CbrAB/Crc carbon catabolite control system revealed by transcript abundance in *Pseudomonas aeruginosa*. PLoS One 7:24. https://doi.org/10.1371/journal.pone.0044637.
40. Hill HD, Jr., Reynolds JA, Hill RL. 1977. Purification, composition, molecular weight, and subunit structure of ovine submaxillary mucin. J Biol Chem 252:3791. https://doi.org/10.1016/S0021-9258(17)40321-8.
41. Castric PA. 1977. Glycine metabolism by *Pseudomonas aeruginosa*: hydrogen cyanide biosynthesis. J Bacteriol 130:826. https://doi.org/10.1128/jb.130.2.826-831.1977.
42. Rai RK, Azim A, Sinha N, Sahoo JN, Singh C, Ahmed A, Saigal S, Baronia AK, Gupta D, Gurjar M, Poddar B, Singh RK. 2013. Metabolic profiling in human lung injuries by high-resolution nuclear magnetic resonance spectroscopy of bronchoalveolar lavage fluid (BALF). Metabolomics 9:667–676. https://doi.org/10.1007/s11306-012-0472-y.
43. Camus L, Briaud P, Bastien S, Elsen S, Doléans-Jordheim A, Vandenesch F, Moreau K. 2020. Trophic cooperation promotes bacterial survival of *Staphylococcus aureus* and *Pseudomonas aeruginosa*. Isme J 14:3093–3105. https://doi.org/10.1038/s41396-020-00741-9.
44. Scott J, Sueiro-Olivares M, Ahmed W, Heddergott C, Zhao C, Thomas R, Bromley M, Latgé JP, Krappmann S, Fowler S, Bignell E, Amich J. 2019. *Pseudomonas aeruginosa*-derived volatile sulfur compounds promote distal *Aspergillus fumigatus* growth and a synergistic pathogen-pathogen interaction that increases pathogenicity in co-infection. Front Microbiol 10:2311. https://doi.org/10.3389/fmicb.2019.02311.
45. Briaud P, Bastien S, Camus L, Boyadjian M, Reix P, Mainguy C, Vandenesch F, Doléans-Jordheim A, Moreau K. 2020. Impact of coexistence phenotype between *Staphylococcus aureus* and *Pseudomonas aeruginosa* isolates on clinical outcomes among cystic fibrosis patients. Front Cell Infect Microbiol 10:266. https://doi.org/10.3389/fcimb.2020.00266.
46. Keown K, Reid A, Moore JE, Taggart CC, Downey DG. 2020. Coinfection with *Pseudomonas aeruginosa* and *Aspergillus fumigatus* in cystic fibrosis. Eur Respir Rev 29:200011. https://doi.org/10.1183/16000617.0011-2020.
47. Heurlier K, Dénervaud V, Pessi G, Reimmann C, Haas D. 2003. Negative control of quorum sensing by RpoN (sigma54) in *Pseudomonas aeruginosa* PAO1. J Bacteriol 185:2227. https://doi.org/10.1128/JB.185.7.2227-2235.2003.
48. Lloyd MG, Lundgren BR, Hall CW, Gagnon LB, Mah TF, Moffat JF, Nomura CT. 2017. Targeting the alternative sigma factor RpoN to combat virulence in *Pseudomonas aeruginosa*. Sci Rep 7:12615. https://doi.org/10.1038/s41598-017-12667-y.
49. Coffey BM, Anderson GG. 2014. Biofilm formation in the 96-well microtiter plate. Methods Mol Biol 1149:631–641. https://doi.org/10.1007/978-1-4939-0473-0_48.
50. Comolli JC, Hauser AR, Waite L, Whitchurch CB, Mattick JS, Engel JN. 1999. *Pseudomonas aeruginosa* gene products PilT and PilU are required for cytotoxicity in vitro and virulence in a mouse model of acute pneumonia. Infect Immun 67:3625–3636. https://doi.org/10.1128/IAI.67.7.3625-3630.1999.
51. Yang F, Zhang J, Yang Y, Ruan F, Chen X, Guo J, Abdel-Razek O, Zuo YY, Wang G. 2020. Regulatory roles of human surfactant protein B variants on genetic susceptibility to *Pseudomonas aeruginosa* pneumonia-induced sepsis. Shock 54:507–519. https://doi.org/10.1097/SHK.0000000000001494.
52. Ge L, Liu X, Chen R, Xu Y, Zuo YY, Cooney RN, Wang G. 2016. Differential susceptibility of transgenic mice expressing human surfactant protein B genetic variants to *Pseudomonas aeruginosa* induced pneumonia. Biochem Biophys Res Commun 469:171. https://doi.org/10.1016/j.bbrc.2015.11.089.
53. Xu Y, Ge L, Abdel-Razek O, Jain S, Liu Z, Hong Y, Nieman G, Johnson F, Golub LM, Cooney RN. 2016. Differential susceptibility of human Sp-B genetic variants on lung injury caused by bacterial pneumonia and the effect of a chemically modified curcumin. Shock 45:375. https://doi.org/10.1097/SHK.0000000000000535.
54. Liu J, Abdel-Razek O, Liu Z, Hu F, Zhou Q, Cooney RN, Wang G. 2015. Role of surfactant proteins A and D in sepsis-induced acute kidney injury. Shock 43:31. https://doi.org/10.1097/SHK.0000000000000270.
55. Du J, Abdel-Razek O, Shi Q, Hu F, Ding G, Cooney RN, Wang G. 2018. Surfactant protein D attenuates acute lung and kidney injuries in pneumonia-induced sepsis through modulating apoptosis, inflammation and NF-κB signaling. Sci Rep 8:15393. https://doi.org/10.1038/s41598-018-33828-7.